Anomalous Hall effect in two-phase semiconductor structures: The role of ferromagnetic inclusions

A. V. Kudrin,[1,*] A. V. Shvetsov,[1] Yu. A. Danilov,[1] A. A. Timopheev,[2] D. A. Pavlov,[1] A. I. Bobrov,[1] N. V. Malekhonova,[1] and N. A. Sobolev[2]

[1]*Department of Physics, Lobachevsky State University of Nizhny Novgorod, Nizhny Novgorod 603950, Russia*

[2]*Department of Physics, I3N, University of Aveiro, Aveiro 3810-193, Portugal*

(Received 22 May 2014; published 21 July 2014)

The Hall effect in InMnAs layers with MnAs inclusions of 20–50 nm in size is studied both theoretically and experimentally. We find that the anomalous Hall effect can be explained by the Lorentz force caused by the magnetic field of ferromagnetic inclusions and by an inhomogeneous distribution of the current density in the layer. The hysteretic dependence of the average magnetization of ferromagnetic inclusions on an external magnetic field results in a hysteretic dependence of $R_H(H_{ext})$. Thus, we show the possibility of a hysteretic $R_H(H_{ext})$ dependence (i.e., observation of the anomalous Hall effect) in thin conductive layers with ferromagnetic inclusions in the absence of carriers' spin polarization.

DOI: 10.1103/PhysRevB.90.024415 PACS number(s): 72.20.My, 61.72.uj, 72.25.Dc, 75.50.Pp

The investigation of the anomalous Hall effect (AHE) is a widely used experimental method for the diagnostics of the magnetic and transport properties of ferromagnetic layers, in particular, those of diluted magnetic semiconductors (DMSs) [1]. In the conventional interpretation, the AHE is a consequence of an asymmetric scattering of spin-polarized charge carriers in ferromagnetic materials [2]. Thus, the observation of the AHE is traditionally considered to be a proof of the presence of spin-polarized carriers. The spin polarization of carriers in DMSs is usually attributed to a mechanism of indirect exchange interaction between transition-metal ions via charge carriers [3,4]. In the high-temperature region this mechanism should become slack [3,4]. However, the AHE was observed at room temperature or above in some Mn-doped semiconductors [5–7]. The AHE was also observed at about 300 K in Co-doped TiO_2 [8,9] and $(La,Sr)TiO_3$ [10] layers containing Co clusters. In Refs. [8–10] the appearance of the AHE was related to spin polarization by extrinsic (induced by the clusters) spin-orbit scattering. Earlier, it was also observed that in InMnAs layers obtained by laser deposition in a gas atmosphere a clear hysteresis in the magnetic-field dependencies of the Hall resistance manifests itself up to room temperature [11,12]. In addition, the AHE was observed at high temperatures in the hybrid system consisting of self-organized GeMn nanocolumns in a $Ge_{1-x}Mn_x$ layer [13]. Modeling magnetotransport in such structures revealed that the manifestation of the AHE can be explained by two reasons: a strong difference in the longitudinal resistivity of the matrix and the nanocolumns and large values of the transverse resistivity of the nanocolumns [14]. Thus, the AHE in this hybrid system was associated with a strong anomalous Hall effect within the nanocolumns (with large values of the extraordinary Hall coefficient in GeMn inclusions that is much larger that the ordinary Hall coefficient in a Ge matrix). This consideration was carried out under the condition that the spin-diffusion length of the carriers was shorter than the distance between the nanocolumns which were about 5–10 nm [13,14]. Such an assumption is justified for high temperatures.

In this paper, we present the results of theoretical and experimental investigations of the AHE in the InMnAs layers obtained by laser deposition. Nevertheless our results can be generalized for other conductive layers with ferromagnetic inclusions. The InMnAs layers were grown by the pulsed laser sputtering of semiconductor InAs and metallic Mn targets placed in the quartz reactor with flows of hydrogen (the carrier gas) and arsine (the arsenic source) [15]. Semi-insulating GaAs (100) was used as a substrate. The layers were grown at 320 °C. The content of Mn was characterized by the technological parameter $Y_{Mn} = t_{Mn}/(t_{Mn} + t_{InAs})$, where t_{Mn} and t_{InAs} are the ablation times of the Mn and InAs targets. Structural properties were investigated by high-resolution cross-sectional transmission electron microscopy. The distribution of constituent elements was obtained by the energy-dispersive x-ray spectroscopy (EDS). The dc magnetotransport measurements were carried out in a van der Pauw geometry from 10 to 300 K in a closed-cycle He cryostat.

In III-Mn-V layers the second-phase inclusions may appear during technology processes. In particular, nanosize ferromagnetic MnAs particles can be embedded in a semiconductor GaAs [16,17] and InAs [18] matrix. The presence of an MnAs phase in the InMnAs layers grown by laser deposition was revealed by x-ray-diffraction studies [11,12]. The temperature dependences of the ferromagnetic resonance [12] and magnetization [19] for the InMnAs layers show a Curie temperature of about 330 K that is close to the Curie temperature for MnAs. The $R_H(H_{ext})$ dependences become linear also at the temperature of about 330 K that indicates the connection of the AHE with ferromagnetic properties of the MnAs inclusions. It was shown in Ref. [12] that an increase in the Mn content (Y_{Mn}) leads to a reinforcement of the hysteretic character of the $R_H(H_{ext})$ dependences.

Figure 1 shows the bright-field cross-sectional scanning transmission electron microscopy (STEM) image of the InMnAs/GaAs structure with $Y_{Mn} = 0.2$. The image reveals a phase inhomogeneity of the InMnAs layer. Figure 1 also shows the energy-dispersive EDS mapping of Mn, In, and As in the structure. The bright areas in the Mn mapping image correspond to the regions of predominantly Mn atoms. At the same time these regions are free from In atoms. Taking into account the uniform distribution of As atoms it can be

*kudrin@nifti.unn.ru

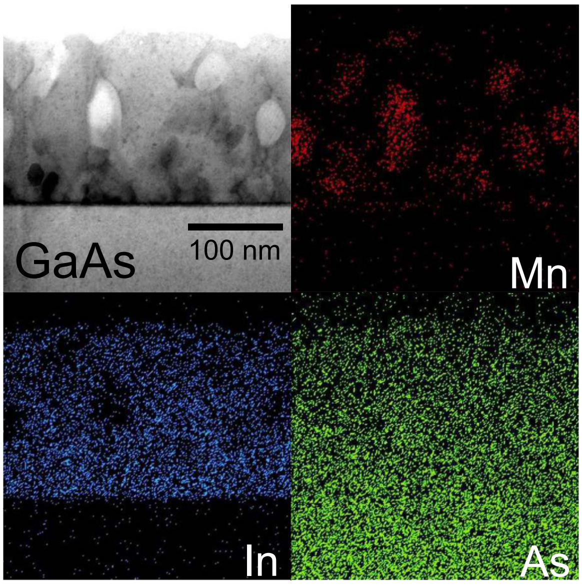

FIG. 1. (Color online) The bright-field STEM image of the InMnAs/GaAs structure (upper left). The corresponding EDS mappings for Mn, In, and As.

concluded that the bright areas in the Mn mapping image correspond to the inclusions of a MnAs phase. Thus, the InMnAs layers contain MnAs clusters of 20–50-nm size.

Let us assume that the semiconductor matrix has no magnetic ordering at the temperatures considered (200–300 K) and the charge carriers have no predominant spin polarization. This assumption is based on the theory of carrier-mediated ferromagnetism which demands much higher carrier concentrations for the appearance of a ferromagnetic ordering in DMSs than those found in our InMnAs layers (6×10^{15}–5×10^{18} cm^{-3} as will be shown below). In this case the magnetic properties of this structure are determined only by the ensemble of ferromagnetic MnAs inclusions. We also neglect the possible presence of any spin-dependent processes, even if the magnetic nanoparticles participate in the transport of electric charges.

The Lorentz force arises from the interaction of the magnetic fields of the ferromagnetic nanoparticles and the movements of the charge carriers. Moreover, an inhomogeneous distribution of the current density should be observed due to the layer heterogeneity. The principal idea of this paper is to show that such a simple model is sufficient to describe qualitatively and quantitatively the hysteretic dependences of the Hall resistance on an external magnetic field in a conductive nonmagnetic matrix containing ferromagnetic inclusions, without taking into consideration any spin-related phenomena.

The magnetic properties of an ensemble of ferromagnetic particles are dependent mainly on the magnetic anisotropy of particle K and particle volume V_p. These parameters define a blocking temperature T_B of the ensemble which separates the superparamagnetic state from the blocked one according to the relationship [20] $T_B = KV_p/25k_B$, where k_B is the Boltzmann constant. As in Ref. [21], MnAs has an "easy-plane" magnetocrystalline anisotropy for which T_B should be 0 K. Thus, it cannot provide the blocked character of

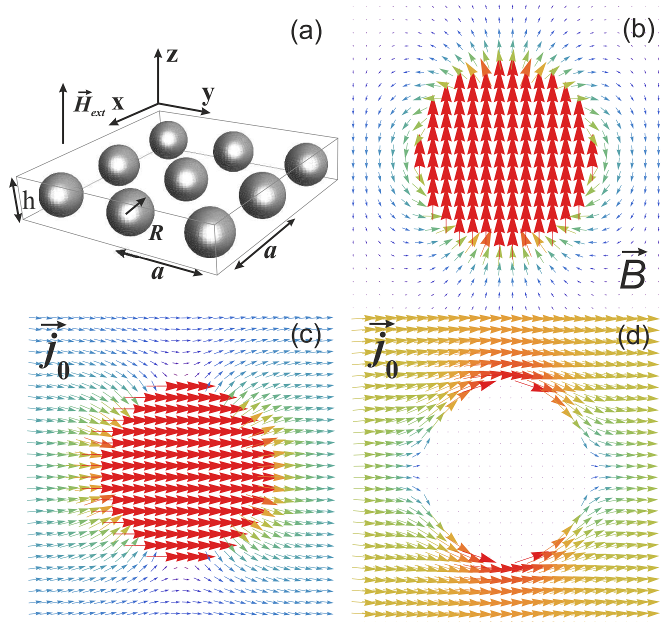

FIG. 2. (Color online) (a) The two-dimensional lattice of spherical ferromagnetic particles (a is the interparticle distance, and R is the radius of the particles). (b) The distribution of the magnetic induction $\vec{B}$ across the layer. (c) The current lines for the case of particles with high conductivity. (d) The current lines for the case of particles with low conductivity.

the magnetization reversal with the coercivity $H_C \sim 0.5$ kOe as was observed for our InMnAs layers [12,19] as well as for 20–100-nm-size MnAs clusters embedded in a GaAs matrix [16,17]. At the same time, the particles have an elongated shape (see Fig. 1), and in our case it is apparently the main source of the magnetic hysteresis. The microscopy revealed that the typical particle shape is an ellipsoid with the axes $a \simeq b \simeq c/2$. This results in the effective uniaxial anisotropy constant $K \simeq 5 \times 10^5$ erg/cm^3 for $M_S = 600$ emu/cm^3 (Ref. [21]). So, to be unblocked at room temperature, the particle size must be less than 15 nm. The observed particles are several times larger than this (Fig. 1). Therefore the considered ensemble of the MnAs nanoparticles is in the blocked state at room temperature and thus possesses a coercivity.

In the z direction (normal to the layer plane), the film contains one or a few MnAs particles (Fig. 1). Thus, a two-dimensional lattice of spherical ferromagnetic particles can be taken as the simplest model of the considered system [Fig. 2(a)]. If the system is classically described and there is no barrier for carriers at the particle/matrix interface, then the half-metallic MnAs particles in a semiconductor matrix can be considered as a region with enhanced conductivity. We assume that a current flows in the y direction, then the current density outside the particle is

$$\vec{j} = \vec{j}_0\left(1 - \frac{R^3}{r^3}\frac{\sigma_1 - \sigma_2}{\sigma_1 + 2\sigma_2}\right) + \frac{\sigma_1 - \sigma_2}{\sigma_1 + 2\sigma_2}\frac{3j_0R^3y\vec{r}}{r^5}, \quad (1)$$

whereas the current density inside the particle is

$$\vec{j} = \frac{3\sigma_1}{\sigma_1 + 2\sigma_2}\vec{j}_0, \quad (2)$$

where $\vec{j}_0$ denotes the current density far from a particle. The origin of coordinates is in the center of a particle. The conductivity of the semiconductor matrix is characterized by a value of σ_2, and the conductivity of the particle is σ_1. Since $\sigma_1 > \sigma_2$, the current lines are involved into the particle as shown in Fig. 2(c), and the current density in the particle is distinctly higher than far from it. On the other hand the particle/matrix interface can be a barrier for carriers. Consequently the particle can be considered as a region with low effective conductivity ($\sigma_1 < \sigma_2$), and the current flow will bend around the inclusion [Fig. 2(d)]. In the limiting case when the barrier is impenetrable, charge carriers move in a space between the inclusions in a magnetic field produced by the inclusions and in an external magnetic field. It will be shown hereafter that, regardless of whether there is a barrier or it is absent, the hysteretic dependence of the Hall resistance on an external magnetic field [$R_H(H_{ext})$] will be observed. This is attributed to the system heterogeneity and to the hysteretic dependence of the inclusion magnetization on an external magnetic field.

For the layer in the external magnetic field $\vec{H}_{ext}$ applied along the z direction the average force acting on carriers per unit volume is defined as

$$\vec{F} = \frac{1}{\Delta V}\int_{\Delta V}\frac{1}{c}[\vec{j}\times\vec{B}]dV, \tag{3}$$

where $\Delta V = ha^2$ is the volume of the layer per ferromagnetic particle. Assuming that all the particles are uniformly magnetized along the z direction each particle produces the magnetic field at point $\vec{r}_i$ equal to

$$\vec{H}_i = \frac{3(\vec{m}\vec{r}_i)\vec{r}_i}{r_i^5} - \frac{\vec{m}}{r_i^3}, \tag{4}$$

where $\vec{m} = (4/3)\pi R^3\vec{M}_0$ is the magnetic moment of the particle and $\vec{M}_0$ is the magnetization of the latter. The particle with the number j is subject to the external magnetic field $\vec{H}_{ext}$ and the fields of the other particles (4). Assuming that distance a between the particles noticeably exceeds R the field produced by all other particles near the jth particle can be considered as locally homogeneous $\vec{H}_p \simeq -(2\pi h/a)\vec{M}_0\vartheta$, where ϑ is the volume fraction of the ferromagnetic inclusions. Consequently, the field inside each particle is

$$\vec{H} \simeq \vec{H}_{ext} + \vec{H}_p - (4/3)\pi\vec{M}_0. \tag{5}$$

The field in the space between the particles cannot be considered as homogeneous, but hereinafter we will use only the average value of the field. Since the volume per particle is ha^2 and all the particles are identical, we find the average field $\bar{H}_z$ in the space between the particles using the superposition principle,

$$\bar{H}_z = H_{ext} + \frac{1}{ha^2}\int_V H_{i,z}dV, \tag{6}$$

where integration is over the layer volume. The substitution of $\vec{H}_i$ Eq. (4) into Eq. (6) yields

$$\bar{H}_z = H_{ext} - \frac{8\pi}{3}M_0\vartheta, \tag{7}$$

and $\bar{H}_x = \bar{H}_y = 0$ owing to the problem symmetry.

Let us examine two limit cases. (i) Let a barrier for carriers at the particle/matrix interface be present, so $\sigma_1 \ll \sigma_2$. In this case as follows from Eq. (2) $\vec{j} \sim (\sigma_1/\sigma_2)\vec{j}_0 \approx 0$, and the current flow does not penetrate into the inclusion. Therefore the charge carriers move in the space between the inclusions in the average field $\bar{H}_z$ Eq. (6). (ii) If the barrier is absent, then $\sigma_1 \gg \sigma_2$. Hence the current density in the particle is $\vec{j} \simeq 3\vec{j}_0$ [Eq. (2)], and the current flow is involved into the particle. In this case carriers inside the particle are subject to the magnetic field Eq. (5). For case (i) the average Lorentz force can be approximately found according to Eqs. (3) and (7) as

$$F_x \simeq \frac{1}{ha^2}\int_{V_m}\frac{1}{c}j_0\bar{H}_z dV = -\frac{8\pi}{3c}j_0M_0\vartheta + \frac{1}{c}j_0H_{ext}(1-\vartheta), \tag{8}$$

and for case (ii) according to Eqs. (3), (5), and (7) as

$$\begin{aligned} F_x \simeq{}& \frac{1}{ha^2c}\left[\int_{V_p}3j_0\left(H_{ext}+H_p+\frac{8\pi}{3}M_0\right)dV \right.\\ &\left. +\int_{V_m}j_0\bar{H}_z dV\right]\\ \simeq{}& \frac{16\pi}{3c}j_0M_0\vartheta + \frac{1}{c}j_0(1+2\vartheta)H_{ext}, \end{aligned} \tag{9}$$

where V_p is the particle volume and $V_m = ha^2 - V_p$. According to Eqs. (8) and (9), the average Lorentz force depends on the magnetization of the particles. It should be noted that for case (i) the sign of the first term in Eq. (8) is different from that for case (ii) Eq. (9). This will be discussed in more detail hereafter. The MnAs inclusions are ferromagnetic, and the hysteretic dependence of magnetization M_0 on the external magnetic field leads to a hysteretic dependence of the Hall resistivity on the external magnetic field $\rho_H(H_{ext}) = F_x(H_{ext})/(enj_0)$, where n is the charge-carrier concentration in the semiconductor matrix and e is the electron charge. According to Eqs. (8) and (9) the remanent Hall resistance is

$$R_H(H_{ext}=0) \simeq \gamma\frac{8\pi}{3}\frac{M_0\vartheta}{hnec}, \tag{10}$$

where $\gamma = 1$ for $\sigma_1 \ll \sigma_2$ and $\gamma = 2$ for $\sigma_1 \gg \sigma_2$. As an estimation of M_0 we take the value of the remanent magnetization of an epitaxial MnAs layer (about 900 G at 270 K [22]). The typical value of the carrier concentration for our InMnAs layers at 270 K is about 3×10^{18} cm^{-3}, and the layer thickness is $h \simeq 190$ nm. For the volume the fraction of MnAs inclusions in the InMnAs layer is about 0.05 (Fig. 1), and the value of $R_H(H_{ext}=0)$ equals approximately 0.5 Ω, which is in good agreement with the experimental results (Fig. 3).

Since for the discussed model the hysteresis in the $R_H(H_{ext})$ dependence is due to the Lorentz force, it can be attributed to the ordinary Hall effect (OHE). Consequently, for a fixed volume fraction and a magnetization value of the MnAs particles in the layer, the value of the remanent Hall resistance should increase with decreasing the carrier concentration, in accordance with Eq. (10).

It is known that the ion irradiation can vary the carrier concentration in semiconductors due to the formation of radiation-induced crystal defects. A feature of the InAs semiconductor is that radiation defects shift the Fermi level toward the conduction band, which leads to an increase in the

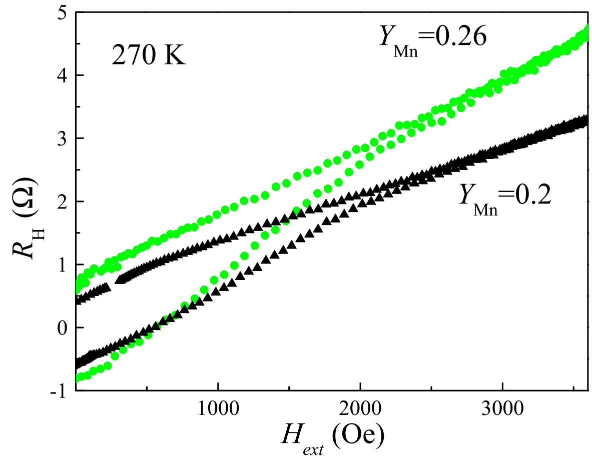

FIG. 3. (Color online) The $R_H(H_{ext})$ dependences at 270 K for the InMnAs layer with manganese content $Y_{Mn} = 0.2$ (black triangles) and $Y_{Mn} = 0.26$ (red circles).

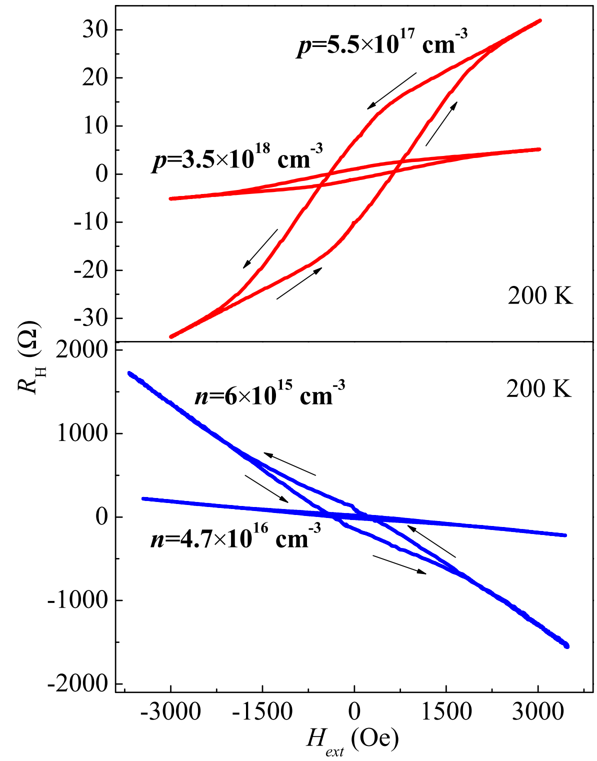

FIG. 4. (Color online) The $R_H(H_{ext})$ dependences at 200 K for the InMnAs layer ($Y_{Mn} = 0.2$) for the different carrier-concentration values. The arrows indicate the magnetic-field scan directions.

carrier concentration in the n-type material or the p-n-type conversion in p-InAs (Ref. [23]). To change the carrier concentration in the InMnAs layer, the proton implantation was carried out with an energy of 50 keV and a fluence in the range of 1×10^{13}–6×10^{14} cm^{-2}. Table I shows the values of the carrier concentration and the mobility at 300 and 200 K in the InMnAs layer with $Y_{Mn} = 0.2$ before and after irradiations with different proton fluences. The values of the carrier concentration were determined from the slope of the $R_H(H_{ext})$ dependences in H_{ext} above 3000 Oe, i.e., mainly in the linear region. The temperature of 200 K was the lowest one at which it was possible to obtain the $R_H(H_{ext})$ dependences for a high-resistance layer irradiated by protons with a fluence of 1×10^{14} cm^{-2}.

Proton implantations with fluences of 1×10^{13} and 3×10^{13}cm^{-2} lead to a decrease in the concentration of carriers (holes) as a result of the partial compensation of the Mn acceptor impurity by radiation-induced donor-type defects (Table I). The conversion of the conductivity type from p to n is observed after the implantation with a fluence of 1×10^{14} cm^{-2}. With a further increase in the proton fluence to 6×10^{14} cm^{-2} the concentration of the majority carriers (electrons) rises (Table I). We suppose that the proton implantation with relatively low fluence (1×10^{13}–6×10^{14} cm^{-2}) does not lead to a significant modification of properties of the half-metallic MnAs inclusions, and the magnetic properties of the inclusions remain invariable. In the frame of this assumption and in accordance with our model we can conclude that the change in $R_H(H_{ext} = 0)$ value after the proton implantation is related to the change in the carrier concentration.

Figure 4 shows the $R_H(H_{ext})$ dependences at 200 K for the InMnAs layer with different carrier-concentration values. For a fixed H_{ext} the Hall resistance value of the linear part of the $R_H(H_{ext})$ dependence increases with decreasing carrier concentration. This is typical for the OHE and is related to the increase in the Hall coefficient $R_0 = 1/en$. We emphasize that both for the cases of the p- and n-type majority carriers the clear increase in the remanent Hall resistance with decreasing carrier concentration is also observed (Fig. 4). So, the experimental results are in good agreement with our model: the $R_H(H_{ext} = 0)$ value increases with decreasing carrier concentration.

Figure 5 exhibits the hysteretic component of the $R_H(H_{ext})$ dependences at 200 K for the InMnAs layer before and

TABLE I. The concentration of charge carriers and the mobility at 300 and 200 K in the InMnAs layer with $Y_{Mn} = 0.2$ before and after implantation of protons with different fluences. In parentheses we indicate the type of majority carriers.

Fluence (cm^{-2})	Carrier concentration at 300 K (cm^{-3})	Carrier mobility at 300 K (cm^2 V^{-1} s^{-1})	Carrier concentration at 200 K (cm^{-3})	Carrier mobility at 200 K (cm^2 V^{-1} s^{-1})
0	4.8×10^{18} (p)	21	3.5×10^{18} (p)	26
1×10^{13}	3.5×10^{18} (p)	21	2.3×10^{18} (p)	27
3×10^{13}	9.8×10^{17} (p)	22	5.5×10^{17} (p)	23
1×10^{14}	2.7×10^{16} (n)	220	6.0×10^{15} (n)	120
2×10^{14}	1.0×10^{17} (n)	260	4.7×10^{16} (n)	160
6×10^{14}	1.6×10^{17} (n)	490	9.0×10^{16} (n)	420

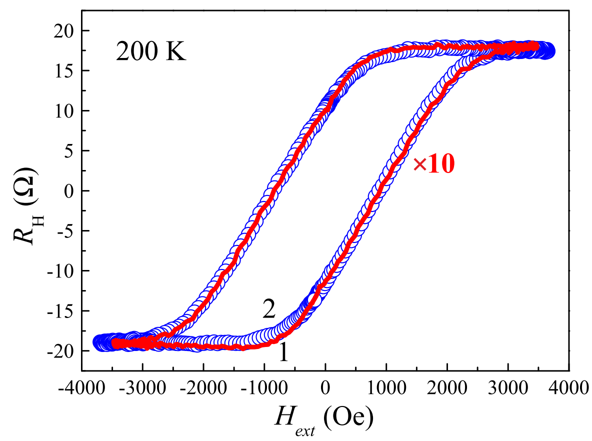

FIG. 5. (Color online) The hysteretic component of the $R_H(H_{ext})$ dependences at 200 K for the InMnAs layer before proton irradiation (dependence 1, red line) and after irradiation with proton fluence 6×10^{14} cm^{-2} (dependence 2, blue circles). The dependence for the nonirradiated InMnAs layer was multiplied by 10.

after irradiation with a proton fluence of 6×10^{14} cm^{-2}. The dependences were obtained by subtracting the linear part of the $R_H(H_{ext})$ dependencies. As can be seen, the shape of the hysteretic component remains the same. This confirms our assumption that carried out proton implantation does not lead to a significant modification in the magnetic properties of the MnAs inclusions.

Figure 6 shows the experimental dependences of the remanent Hall resistance on the carrier concentration at a temperature of 200 K. Since for the OHE the Hall resistance is inversely proportional to the carrier concentration, the dependence of the remanent Hall resistance on the concentration in the double-logarithmic coordinates should be linear (Fig. 6). The linear approximation of the experimental points is shown in Fig. 6. The slope coefficients are sufficiently close to unity (as shown in Fig. 6), which corresponds to the assumption about the determinative role of the OHE [Eq. (10)] in the observed hysteretic dependences $R_H(H_{ext})$. We note that for a fixed carrier concentration the remanent Hall resistance will be higher for the p-type carriers than for the n-type

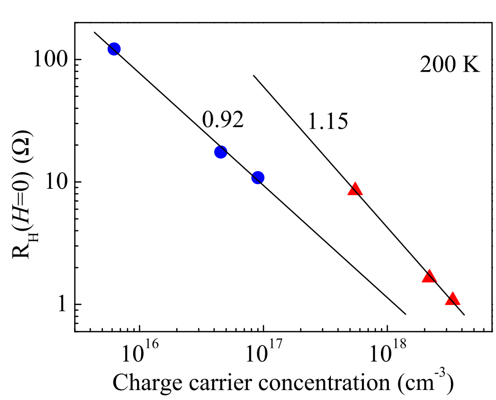

FIG. 6. (Color online) The experimental dependences of the remanent Hall resistance on the hole concentration (triangles) and electron concentration (circles). The solid lines show linear approximations of the experimental data.

carriers (Fig. 6). This effect has been predicted by the proposed model. It follows from Eqs. (8)–(10) that in the case when the conductivity of the inclusions is higher than that of the matrix, the influence of the magnetic field of the inclusions on the Hall effect will be two times higher than in the opposite case. Thus, it is possible to conclude that for holes the barrier at the cluster/matrix interface is absent. However for electrons an impenetrable barrier at the cluster/matrix interface is present, which causes their predominant movement in the InMnAs layer between the MnAs clusters. It is known that MnAs is a p-type ferromagnetic half-metal [24]. This is in good agreement with our conclusion about the presence of a barrier for electrons between the InMnAs matrix and the MnAs cluster.

It should be noted that, for p-type carriers, the sign of the linear component of the $R_H(H_{ext})$ dependencies coincides with the sign of the hysteretic component. For n-type carriers these components have a different sign (Fig. 4). The difference between the signs of the linear component is related to the different type of carriers. At the same time, both for the p- and for the n-type majority carriers the sign of the hysteretic component is the same (Fig. 4). The reason for that is the following. As discussed hereinabove, for holes the MnAs inclusions are the regions with enhanced conductivity [Fig. 2(c)]. For this case within the cluster the carriers (holes) are affected by the Lorentz force. This leads to the average Lorentz force given by Eq. (9). Since the direction of the magnetization of the MnAs clusters (at the saturation point) coincides with that of H_{ext} [Fig. 2(b)] the sign of the hysteretic component of the $R_H(H_{ext})$ dependence (which is determined by the magnetization of the MnAs inclusions) is equal to the sign of the linear component which is determined by H_{ext}. In contrast, in n-type layers the majority carriers (electrons) move between the MnAs inclusions in the magnetic field of inclusions and in the external magnetic field. However the magnetic field which is produced by the clusters has the opposite direction to the magnetization of the clusters [Fig. 2(b)] and is consequently opposite to H_{ext}. This leads to the difference in the signs of the terms in Eq. (8) for the average Lorentz force and to the difference in the signs of the linear and hysteretic components of the $R_H(H_{ext})$ dependencies for n-type layers (Fig. 4).

Besides the AHE, the magnetoresistance (MR) was measured for both n- and p-type layers (see Fig. 7). For the case of n-type InMnAs layers (after proton irradiation) a small negative magnetoresistance is observed. The change in resistance is about 0.1%–0.15% in the magnetic field of 4000 Oe and has a weak dependence on the temperature and carrier concentration. In accordance with our assumption electrons do not penetrate into the particles due to the barrier at the particle/matrix interface and therefore move in the InAs matrix. The negative magnetoresistance is typical for strongly compensated n-type InAs and was observed at a wide temperature range (up to room temperature) [25,26]. The negative MR in semiconductors heavily doped with a nonmagnetic impurity was associated with the scattering of carriers on the localized spins [25–27]. For the case of p-type InMnAs layers we observed a very small positive magnetoresistance (Fig. 7) with a weak dependence on temperature. As shown in Ref. [14] for a composite system consisting of magnetic GeMn

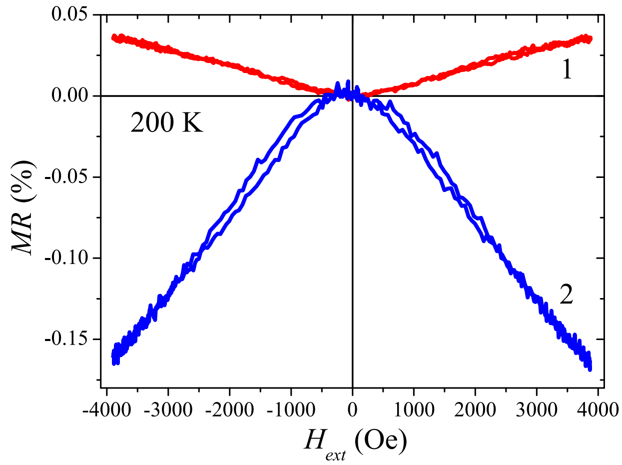

FIG. 7. (Color online) The magnetoresistance at 200 K for the InMnAs layer ($Y_{\mathrm{Mn}} = 0.2$): 1—MR before implantation of protons; 2—MR after the implantation with a fluence of 1×10^{14} cm^{-2}.

columns in a nonmagnetic $\mathrm{Ge}_{1-x}\mathrm{Mn}_x$ matrix in the case of a large contrast in conductivities of columns (c) and matrix (m) $\sigma_c \gg \sigma_m$ and with a large difference in the transverse resistivity $\rho_{c,xy} \gg \rho_{m,xy}$ a positive contribution to the magnetoresistance prevails for relatively small values of H_{ext}. The significant difference in the values of the transverse resistivity leads in the external magnetic field to a noticeable change in the direction of the current lines in the columns and the matrix. In the above-mentioned paper, a large ratio $\rho_{c,xy}/\rho_{m,xy}$ was achieved by large values of the ratio R_s/R_0, where R_0 and R_s are the extraordinary and ordinary Hall coefficients in the GeMn columns and $\mathrm{Ge}_{1-x}\mathrm{Mn}_x$ matrix, respectively. For our InAs + MnAs hybrid system the model considered in Ref. [14] cannot be directly applied for an explanation of the observed AHE and positive magnetoresistance inasmuch as in contrast to the $\mathrm{Ge}_{1-x}\mathrm{Mn}_x$ system; R_0 in the InAs matrix is much higher (on the order of $10^{-6} - 10^{-3}$ m$^3/C$, Table I) than R_s in the MnAs clusters (on the order of 10^{-7} m$^3/C$, Ref. [24]) therefore $R_s/R_0 \ll 1$. However for our system the positive magnetoresistance can be qualitatively explained by bending of current lines in the external magnetic field in consequence of the difference in the average values of the magnetic fields acting on the charge carriers in the particles and the matrix.

Based on the issues discussed above we can conclude that the apparent AHE in thin conductive layers with ferromagnetic inclusions can be related to the influence of local magnetic fields produced by the inclusions of charge carriers and to an inhomogeneous distribution of the current density in the layer. Thus, we have demonstrated the possibility of the observation of a pronounced anomalous Hall effect in the absence of the spin polarization of charge carriers.

The authors thank B. N. Zvonkov for the growth of the samples and V. K. Vasiliev for the proton implantation. We acknowledge support from RFBR (Grant No. 12-07-00433-a), the Ministry of Education and Science of Russian Federation (Projects No. 3.285.2014/K and No. 8.1054.2014/K), FCT through Grant No. RECI/FIS-NAN/0183/2012 and by the European project Mold-Nanonet.

[1] H. S. Hsu, C. P. Lin, S. J. Sun, and H. Chou, Appl. Phys. Lett. **96**, 242507 (2010).
[2] N. Nagaosa, J. Sinova, S. Onoda, A. H. MacDonald, and N. P. Ong, Rev. Mod. Phys. **82**, 1539 (2010).
[3] T. Dietl, H. Ohno, and F. Matsukura, Phys. Rev. B **63**, 195205 (2001).
[4] A. H. Macdonald, P. Schiffer, and N. Samarth, Nature Mater. **4**, 195 (2005).
[5] X. Chen, M. Na, M. Cheon, S. Wang, H. Luo, B. D. McCombe, X. Liu, Y. Sasaki, T. Wojtowicz, J. K. Furdyna, S. J. Potashnik, and P. Schiffer, Appl. Phys. Lett. **81**, 511 (2002).
[6] N. D. Parashar, N. Rangaraju, V. K. Lazarov, S. Xie, and B. W. Wessels, Phys. Rev. B **81**, 115321 (2010).
[7] J.-H. Yao, H.-H. Lin, Y.-L. Soo, T.-S. Wu, J.-L. Tsai, M.-D. Lan, and T.-S. Chin, Appl. Phys. Lett. **100**, 092404 (2012).
[8] S. R. Shinde, S. B. Ogale, J. S. Higgins, H. Zheng, A. J. Millis, V. N. Kulkarni, R. Ramesh, R. L. Greene, and T. Venkatesan, Phys. Rev. Lett. **92**, 166601 (2004).
[9] Y. J. Lee, M. P. de Jong, W. G. van der Wiel, Y. Kim, and J. D. Brock, Appl. Phys. Lett. **97**, 212506 (2010).
[10] S. X. Zhang, W. Yu, S. B. Ogale, S. R. Shinde, D. C. Kundaliya, W.-K. Tse, S. Y. Young, J. S. Higgins, L. G. Salamanca-Riba, M. Herrera, L. F. Fu, N. D. Browning, R. L. Greene, and T. Venkatesan, Phys. Rev. B **76**, 085323 (2007).
[11] O. V. Vikhrova, Y. A. Danilov, B. N. Zvonkov, A. V. Kudrin, V. V. Podolskii, Y. N. Drozdov, M. V. Sapozhnikov, C. Moura, M. I. Vasilevskiy, and M. P. Temiryazeva, Phys. Solid State **50**, 52 (2008).
[12] Y. A. Danilov, A. V. Kudrin, O. V. Vikhrova, B. N. Zvonkov, Y. N. Drozdov, M. V. Sapozhnikov, S. Nicolodi, E. R. Zhiteytsev, N. M. Santos, M. C. Carmo, and N. A. Sobolev, J. Phys. D: Appl. Phys. **42**, 035006 (2009).
[13] M. Jamet, A. Barski, T. Devillers, V. Poydenot, R. Dujardin, P. Bayle-Guillemaud, J. Rothman, E. Bellet-Amarlic, A. Marty, J. Cibert, R. Mattana, and S. Tatarenko, Nature Mater. **5**, 653 (2006).
[14] I.-S. Yu, M. Jamet, A. Marty, T. Devillers, A. Barski, C. Beigne, P. Bayle-Guillemaud, and J. Cibert, J. Appl. Phys. **109**, 123906 (2011).
[15] B. N. Zvonkov, O. V. Vikhrova, Yu. A. Danilov, P. B. Demina, M. V. Dorokhin, V. V. Podol'skiĭ, E. S. Demidov, Yu. N. Drozdov, and M. V. Sapozhnikov, J. Opt. Technol. **75**, 389 (2008).
[16] J. De Boeck, R. Oesterholt, A. Van Esch, H. Bender, C. Bruynseraede, C. Van Hoof, and G. Borghs, Appl. Phys. Lett. **68**, 2744 (1996).
[17] P. J. Wellmann, J. M. Garcia, J.-L. Feng, and P. M. Petroff, Appl. Phys. Lett. **71**, 2532 (1997).

[18] T. Schallenberg and H. Munekata, J. Cryst. Growth **301-302**, 623 (2007).

[19] Y. Danilov, Y. Drozdov, A. Kudrin, O. Vikhrova, B. Zvonkov, M. Sapozhnikov, L. Fetisov, A. Semisalova, and N. Perov, J. Phys.: Conf. Ser. **200**, 062025 (2010).

[20] L. Neel, Ann. Geophys. **5**, 99 (1949).

[21] R. W. De Blois and D. S. Rodbell, J. Appl. Phys. **34**, 1101 (1963).

[22] P. Xu, J. Lu, L. Chen, S. Yan, H. Meng, G. Pan, and J. Zhao, Nanoscale Res. Lett. **6**, 125 (2011).

[23] V. N. Brudnyi, S. N. Grinyaev, and N. G. Kolin, Physica B **348**, 213 (2004).

[24] J. J. Berry, S. J. Potashnik, S. H. Chun, K. C. Ku, P. Schiffer, and N. Samarth, Phys. Rev. B **64**, 052408 (2001).

[25] U. Garyagdyev, O. V. Emel'yanenko, N. Zotova, T. S. Lagunova, and D. N. Nasledov, Sov. Phys. Semicond. **7**, 487 (1973).

[26] U. Garyagdyev, O. V. Emel'yanenko, N. Zotova, T. S. Lagunova, D. N. Nasledov, and A. V. Pentsov, Sov. Phys. Semicond. **8**, 214 (1974).

[27] Y. Toyozawa, J. Phys. Soc. Jpn. **17**, 986 (1962).